

Cite this: DOI: 10.1039/c0xx00000x

www.rsc.org/ees

## Supplementary Information

### Tuning microcavities in thermally rearranged polymer membrane for CO<sub>2</sub> capture

Sang Hoon Han,<sup>a,c</sup> Hye Jin Kwon,<sup>a</sup> Keun Young Kim,<sup>a</sup> Jong Geun Seong,<sup>b</sup> Chi Hoon Park,<sup>b</sup> Seungju Kim,<sup>a</sup> Cara M. Doherty,<sup>c</sup> Aaron W. Thornton,<sup>c</sup> Anita J. Hill,<sup>c,d</sup> Ángel E. Lozano,<sup>e</sup> Kathryn A. Berchtold,<sup>f</sup>  
5 Young Moo Lee<sup>\*a,b</sup>

Received (in XXX, XXX) Xth XXXXXXXXX 20XX, Accepted Xth XXXXXXXXX 20XX

DOI: 10.1039/b000000x

#### Monomer purification and confirmation

10 High purity (99.9+%) bisAPAF was dried overnight in a vacuum oven at 120 °C before use. Two commercial monocyclic acid chlorides were recrystallized under reduced pressure at 120 °C and stored in an inert atmosphere. To synthesize 6FCl, 10g (30 mmol) of 2,2-bis(4-carboxyphenyl) hexafluoropropane (6FOH)  
15 was reacted with 25ml of thionyl chloride in a flask connected with a dean stark trap and a condenser, followed by heating slowly to 90 °C and stirring for 6 hours. The 6FCl solidified under reduced pressure and was washed with hexane, filtered and recrystallized. The final 6FCl was collected as a fine white  
20 powder after vacuum sublimation at 100 °C. Synthesis of this monomer was confirmed by FT-IR spectra, which indicated a distinct peak at 1,780 cm<sup>-1</sup> corresponding to carboxylic acid chloride without any residual peak at 1,704 cm<sup>-1</sup> from carboxylic acid.<sup>1</sup>

25

#### Modeling procedure

Default values of commercial COMPASS force field were used for charge assigning and force field typing in this simulation,<sup>2,3</sup> except oxygen and nitrogen atoms in the PBO ring.  
30 Those atoms were modified from o2a (oxygen, SP2, aromatic, in 5 membered ring) to o (oxygen, generic) and from n2a (nitrogen, SP2, aromatic) to n3a (nitrogen, SP2, aromatic), respectively, due to the rigid coplanar properties of PBO ring. TR-PBO chains with  
50 repeat units were built and energy-minimized. Amorphous models were constructed at 298 K with experimental densities under periodic boundary conditions using the Amorphous Cell module in Material Studio. Due to the rigid structure of TR-PBOs, the option of ramp density from an initial value of 0.3 g cm<sup>-3</sup> was selected to avoid cell generation failure. The cell was  
40 followed by the energy minimization step *via* the smart minimizer method, which is a combination of the steepest descent, conjugated gradient and Newton methods in a cascade, where the convergence levels were set to 1000 kcal mol<sup>-1</sup> Å<sup>-1</sup>, 10 kcal mol<sup>-1</sup> and 0.1 kcal mol<sup>-1</sup>, respectively.

45 Using energy-minimized amorphous cells of TR-PBOs,

molecular dynamic (MD) simulations were performed using a time step of 1.0 fs for equilibrating the cells and obtaining the final stable structures. The Ewald summation method was used to calculate the non-bond interactions (electrostatic and van der  
50 Waals) with an accuracy of 0.01 kcal mol<sup>-1</sup>. The Andersen algorithm set to a collision ratio of 0.1 was used to control the temperature of each cell. Specific MD simulation procedures for each TR-PBO structure are differently designed according to its corresponding thermal treatment protocol as follows: (1) for TR-  
55 β-PBO, NVT (a constant particle number, volume and temperature) MD simulation at 298, 523, 573, 623 and 298 K, successively, for 100 ps at each temperature, (2) for TR-α-PBO, NVT (a constant particle number, volume and temperature) MD simulation at 298, 573, 723 and 298 K, successively, for 100 ps at  
60 each temperature.

#### Positron annihilation lifetime spectroscopy (PALS)

PALS was used to investigate the pore size and relative pore concentration within the PHAs and TR-PBOs. The size of the  
65 free volume elements within the polymers can then be related to the transport properties of the membranes. Long lifetimes were collected by setting the range of the time-to-amplitude converter to 200 ns and removing the coincident unit to increase count rates. Each file consisted of 4.5 × 10<sup>6</sup> integrated counts and a  
70 minimum of 5 files were collected for each sample or at each temperature. The full width at half maximum (FWHM) resolution of the instrument was determined to be 240 ps when measured with <sup>60</sup>Co. The positron source was prepared with 50 μCi of <sup>22</sup>Na which was dried onto 2.54 μm thick Ti foil and required no  
75 background subtraction. The TR membranes were stacked to 2 mm thickness and placed on each side of the positron source. The sample and source were then placed in the vacuum cell and brought to 5 × 10<sup>-4</sup> Pa. The samples were all initially measured at room temperature (20 °C) under vacuum. PALS was also  
80 measured on sample 6fPBO from 30 to 230 °C at 20 or 30 °C intervals and then returned to 30 °C to ensure there were no permanent changes in the free volume due to the heating regime.

The PALS data was deconvoluted using a four component fit

with LTV9 software by fixing the first lifetime ( $\tau_1$ ) to 0.125 ns due to annihilation of the *para*-positronium (*p*-Ps) and freeing the second lifetime ( $\tau_2$ ) to ~0.4 ns due to free annihilation. Therefore two *ortho*-positronium (*o*-Ps) components ( $\tau_3$  and  $\tau_4$ ) were associated with the bimodal porosity of the PHAs and TR-PBOs. The  $\tau_3$  shorter lifetimes were converted to pore sizes using the Tao-Eldrup semi-empirical formula.<sup>4,5</sup>

$$\tau_3^{-1} = 2 \left[ 1 - \frac{r_3}{r_3 + \Delta r} + \frac{1}{2\pi} \sin \left( \frac{2\pi(r_3)}{r_3 + \Delta r} \right) \right] \quad (1)$$

The longer lifetimes and the lifetimes at high temperatures were calculated using the rectangular Tao-Eldrup (RTE) model.<sup>6</sup>

### Polymer characterization

Poly(*o*-hydroxylamide)s (PHAs) have been utilized to obtain

TR-PBOs derived by cyclodehydration processes from various chemical structures by several researches. In this work, the syntheses of precursor PHAs, which would be converted to TR-PBOs in solid state, were performed using the well-known polyamidation technique.<sup>7,8</sup> As depicted in **Scheme 1**, three different di(acid chloride) monomers were reacted with equimolar diamine in bis(*o*-aminophenol) in the presence of pyridine as a base to minimize the effect of HCl produced during the reaction. The reactions were kept at low temperature to avoid gelation of the formed polymers. The polymer solutions were precipitated, filtrated, washed and dried. These PHAs were characterized by <sup>1</sup>H NMR spectra and FT-IR spectra in **Fig. S1(a)**, which indicated a broad absorption band at 3,400 – 3,100 cm<sup>-1</sup> corresponding to amide and hydroxyl groups, a strong amide carbonyl absorption (C=O) at 1,652 cm<sup>-1</sup> and secondary amine absorption (N-H) at 1,540 cm<sup>-1</sup>. The <sup>1</sup>H NMR spectra of the precursor also showed phenolic hydrogen at 10.3 ppm and 10.4 ppm and amide group at 9.7 ppm and 9.8 ppm<sup>9</sup>

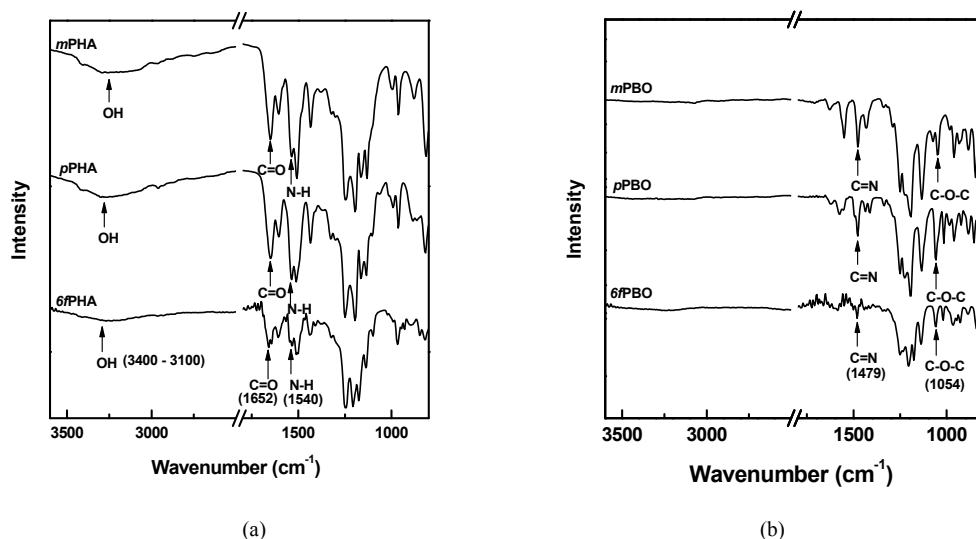


**Fig. S1.** FT-IR spectra of (a) PHAs and (b) TR-β-PBOs

**Table S1.** Elemental analyses of PHAs and TR-PBOs

Polymer structure	Molecular formula of repeating unit	C (wt%)	H (wt%)	N (wt%)	Total (wt%)
PHA	<i>m</i> PHA	C <sub>23</sub> H <sub>14</sub> N <sub>2</sub> O <sub>4</sub> F <sub>6</sub> (55.7)*	2.6 (2.9)*	6.5 (5.7)*	68.9 (64.2)*
	<i>p</i> PHA	C <sub>23</sub> H <sub>14</sub> N <sub>2</sub> O <sub>4</sub> F <sub>6</sub> (55.7)*	3.1 (2.9)*	6.5 (5.7)*	67.9 (64.2)*
	<i>6f</i> PHA	C <sub>32</sub> H <sub>18</sub> N <sub>2</sub> O <sub>4</sub> F <sub>12</sub> (53.2)*	2.8 (2.5)*	4.8 (3.9)*	63.4 (59.6)*
TR-β-PBO	<i>m</i> PBO	C <sub>23</sub> H <sub>10</sub> N <sub>2</sub> O <sub>2</sub> F <sub>6</sub> (60.0)*	1.8 (2.2)*	6.4 (6.1)*	71.7 (68.3)*
	<i>p</i> PBO	C <sub>23</sub> H <sub>10</sub> N <sub>2</sub> O <sub>2</sub> F <sub>6</sub> (60.0)*	1.9 (2.2)*	6.3 (6.1)*	71.8 (68.3)*
	<i>6f</i> PBO	C <sub>32</sub> H <sub>14</sub> N <sub>2</sub> O <sub>2</sub> F <sub>12</sub> (56.0)*	1.8 (2.1)*	4.2 (4.1)*	66.4 (62.1)*

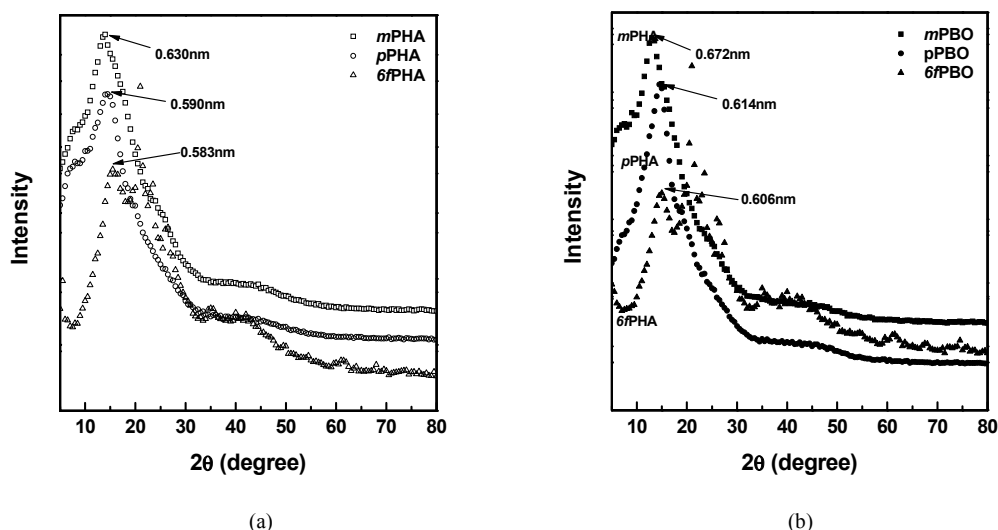


Fig. S2. Wide-angle X-ray diffraction (WAXD) patterns of (a) PHAs ( $\square$ : *m*PHA,  $\circ$ : *p*PHA,  $\triangle$ : *6f*PHA) and (b) TR- $\beta$ -PBOs ( $\blacksquare$ : *m*PBO,  $\bullet$ : *p*PBO,  $\blacktriangle$ : *6f*PBO)

5

Table S2. Cavity diameters and intensities measured by positron annihilation lifetime spectroscopy (PALS)<sup>a</sup>

Polymers	Treatment Temperature (°C)	Smaller cavity			Larger cavity		
		Lifetime, $\tau_3$ (ns)	Cavity diameter (nm)	Intensity, $I_3$ (%)	Lifetime, $\tau_4$ (ns)	Cavity diameter (nm)	Intensity, $I_4$ (%)
<i>m</i> PHA	250	$0.82 \pm 0.13$	$0.27 \pm 0.06$	$11.09 \pm 4.12$	$2.51 \pm 0.03$	$0.655 \pm 0.004$	$18.57 \pm 0.45$
<i>m</i> PHBO	300	$0.90 \pm 0.10$	$0.30 \pm 0.04$	$9.93 \pm 1.99$	$2.92 \pm 0.03$	$0.716 \pm 0.004$	$21.97 \pm 0.37$
<i>m</i> PBO	350	$0.99 \pm 0.09$	$0.33 \pm 0.03$	$8.44 \pm 1.05$	$3.03 \pm 0.03$	$0.731 \pm 0.004$	$19.14 \pm 0.48$
<i>p</i> PHA	250	$1.01 \pm 0.11$	$0.34 \pm 0.04$	$8.07 \pm 0.77$	$2.92 \pm 0.04$	$0.716 \pm 0.006$	$16.09 \pm 0.51$
<i>p</i> PHBO	300	$0.96 \pm 0.11$	$0.32 \pm 0.04$	$8.68 \pm 0.90$	$3.13 \pm 0.03$	$0.744 \pm 0.004$	$19.51 \pm 0.44$
<i>p</i> PBO	350	$0.96 \pm 0.06$	$0.32 \pm 0.02$	$9.68 \pm 0.72$	$3.31 \pm 0.03$	$0.767 \pm 0.004$	$21.00 \pm 0.33$
<i>6f</i> PHA	250	$0.85 \pm 0.08$	$0.28 \pm 0.03$	$9.10 \pm 1.34$	$2.80 \pm 0.02$	$0.699 \pm 0.003$	$17.49 \pm 0.22$
<i>6f</i> PHBO	300	$1.22 \pm 0.21$	$0.40 \pm 0.06$	$7.09 \pm 0.49$	$3.60 \pm 0.05$	$0.802 \pm 0.006$	$22.16 \pm 1.00$
<i>6f</i> PBO	350	$1.24 \pm 0.10$	$0.40 \pm 0.03$	$8.88 \pm 0.54$	$3.79 \pm 0.03$	$0.825 \pm 0.004$	$21.54 \pm 0.76$

<sup>a</sup> Measured at 300K

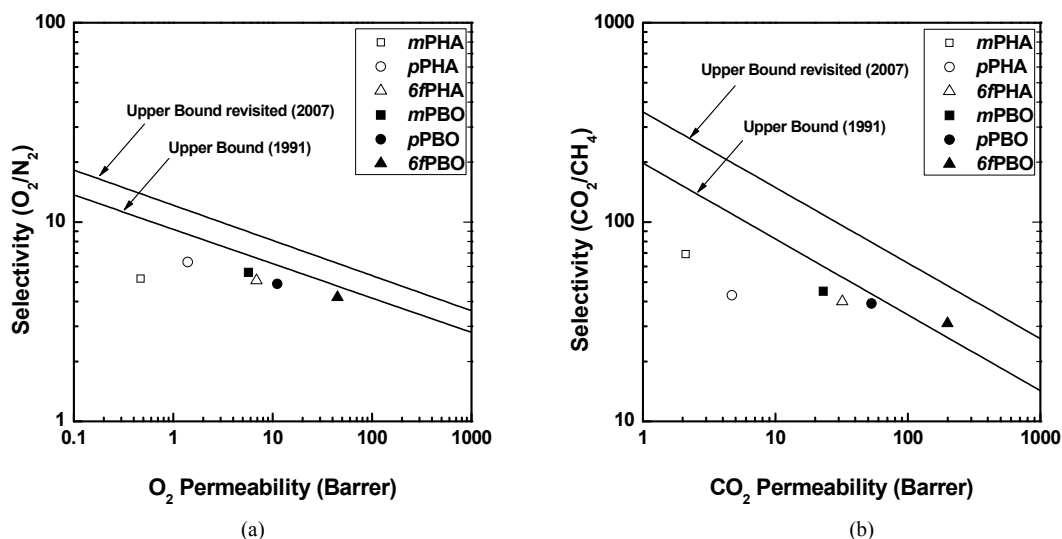


Fig. S3. Trade-off relationships in PHAs and TR- $\beta$ -PBOs for (a)  $O_2/N_2$  and (b)  $CO_2/CH_4$

10

**Table S3.** Gas permeation properties of PHAs and TR- $\beta$ -PBOs at 300K

Polymer Structures	Gas permeability							Ideal selectivity				
	He	H <sub>2</sub>	CO <sub>2</sub>	O <sub>2</sub>	N <sub>2</sub>	CH <sub>4</sub>	H <sub>2</sub> /CO <sub>2</sub>	H <sub>2</sub> /CH <sub>4</sub>	N <sub>2</sub> /CH <sub>4</sub>	O <sub>2</sub> /N <sub>2</sub>	CO <sub>2</sub> /N <sub>2</sub>	CO <sub>2</sub> /CH <sub>4</sub>
<i>m</i> PHA	9.2	5.4	2.1	0.47	0.09	0.03	2.6	180	3.0	5.2	23	69
<i>p</i> PHA	20	14	4.7	1.4	0.2	0.1	3.0	128	2.1	6.3	21	43
<i>6</i> PHA	106	75	32	8.0	1.6	0.81	2.3	93	2.0	5.1	20	40
<i>m</i> PBO	70	60	23	5.7	1.0	0.5	2.6	115	2.0	5.6	23	45
<i>p</i> PBO	82	85	53	11	2.3	1.4	1.6	59	1.6	4.9	23	39
<i>6</i> PBO	251	255	199	45	11	6.4	1.3	40	1.7	4.2	18	31

<sup>a</sup> Pressure: 760 Torr, Temperature: 300K.

## 5 References

1. S. Mehdipour-Ataei and L. Akbarian-Feizi, *Eur. Polym. J.*, 2005, **41**, 1280-1287.
2. J. Yang, Y. Ren, A.-m. Tian and H. Sun, *The Journal of Physical Chemistry B*, 2000, **104**, 4951-4957.
- 10 3. H. Sun, *The Journal of Physical Chemistry B*, 1998, **102**, 7338-7364.
4. S. J. Tao, *J. Chem. Phys.*, 1972, **56**, 5499-5510.
5. M. Eldrup, D. Lightbody and J. N. Sherwood, *Chem. Phys.*, 1981, **63**, 51-58.
6. T. L. Dull, W. E. Frieze, D. W. Gidley, J. N. Sun and A. F. Yee, *J.*
- 15 *Phys. Chem. B*, 2001, **105**, 4657-4662.
7. A. Morisato, K. Ghosal, B. D. Freeman, R. T. Chern, J. C. Alvarez, J. G. de la Campa, A. E. Lozano and J. de Abajo, *J. Membr. Sci.*, 1995, **104**, 231-241.
8. K. I. Okamoto, K. Tanaka, M. Muraoka, H. Kita and Y. Maruyama,
- 20 *J. Polym. Sci., Part B: Polym. Phys.*, 1992, **30**, 1215-1221.
9. S. L.-C. Hsu, K.-S. Lin and C. Wang, *J. Polym. Sci., Part A: Polym. Chem.*, 2008, **46**, 8159-8169.